Translational Oncology
www.transonc.com

Volume 7 Number 2 April 2014 pp. 284–291 284

Ultrasound Targeted Apoptosis Imaging in Monitoring Early Tumor Response of Trastuzumab in a Murine Tumor Xenograft Model of Her-2–Positive Breast Cancer[1]

Xi Wei[*,2], Ying Li[†,2], Sheng Zhang[*,2], Xiujun Gao[‡], Yi Luo[§] and Ming Gao[¶]

*Department of Diagnostic and Therapeutic Ultrasonography, Tianjin Medical University Cancer Institute and Hospital, Key Laboratory of Cancer Prevention and Therapy, Tianjin, China; †The Third Department of Breast Cancer, Tianjin Medical University Cancer Institute and Hospital, Key Laboratory of Cancer Prevention and Therapy, Tianjin, China; ‡Institute of Biomedical Engineering, Tianjin Medical University, Tianjin, China; §Department of Cancer Cell Biology, Tianjin Medical University Cancer Institute and Hospital, Key Laboratory of Cancer Prevention and Therapy, Tianjin, China; ¶Department of Thyroid and Cervical Tumor, Tianjin Medical University Cancer Institute and Hospital, Key Laboratory of Cancer Prevention and Therapy, Tianjin, China

Abstract

OBJECTIVE: Our study aimed to monitor the trastuzumab therapy response of murine tumor xenograft model with human epidermal growth factor receptor 2 (Her-2)–positive breast cancer using ultrasound targeted apoptosis imaging. *METHODS*: We prepared targeted apoptosis ultrasound probes by nanobubble (NB) binding with Annexin V. *In vitro*, we investigated the binding rate of NB–Annexin V with breast cancer apoptotic cells after the trastuzumab treatment. *In vivo*, tumor-bearing mice underwent ultrasound targeted imaging over 7 days. After imaging was completed, the tumors were excised to determine Her-2 and caspase-3 expression by immunohistochemistry (IHC). The correlation between parameters of imaging and histologic results was then analyzed. *RESULTS*: For seeking the ability of targeted NB binding with apoptotic tumor cells (Her-2 positive), we found that binding rate in the treatment group was higher than that of the control group *in vitro* ($P = .001$). There were no differences of tumor sizes in all groups over the treatment process *in vivo* ($P = .98$). However, when using ultrasound imaging to visualize tumors by targeted NB *in vivo*, we observed that the mean and peak intensities from NBs gradually increased in the treatment group after trastuzumab therapy ($P = .001$). Furthermore, these two parameters were significantly associated with caspase-3 expression of tumor excised samples ($P = .0001$). *CONCLUSION:* Ultrasound targeted apoptosis imaging can be a non-invasive technique to evaluate the early breast tumor response to trastuzumab therapy.

Translational Oncology (2014) 7, 284–291

Address all correspondence to: Ming Gao, MD, PhD, Department of Thyroid and Cervical Tumor, Tianjin Medical University Cancer Institute and Hospital, Key Laboratory of Cancer Prevention and Therapy, Huanhuxi Road, Hexi District, Tianjin 300060, China. E-mail: weixi198204@126.com

[1] This study was supported by Tianjin Municipal Health Bureau of Science and Technology Fund (2012 KZ068).
Conflict of interest: No conflicts of interest for all authors.

[2] Xi Wei, Ying Li, and Sheng Zhang contributed equally to this work.

Received 9 January 2014; Revised 5 February 2014; Accepted 6 February 2014

http://dx.doi.org/10.1016/j.tranon.2014.02.015

Introduction

Breast cancer has become the most common cancer for female in urban areas in China [1]. Among them, human epidermal growth factor receptor 2 (Her-2)–positive breast cancers account to 25% to 30%, which have the characteristics of high invasion, early recurrence, and metastasis [2,3]. Trastuzumab is a monoclonal antibody that interferes with Her-2 and highly improves overall survival in late-stage breast cancer [4]. However, the rapid development of drug resistance after 1-year trastuzumab treatment and the high cost have limited its usage [7,8].

To date, there are clinical and traditional imaging techniques for the evaluation of trastuzumab therapy in patients with Her-2–positive breast cancer [4]. However, the measurement of tumor size by the clinical palpation and imaging examinations will not always be good methods for the assessment of therapy response [5,23]. Earlier assessment of trastuzumab effects on Her-2–positive breast cancer before morphologic changes can avoid exposing unnecessary possible side effects and costs from this therapy. Before significant changes in tumor morphologic alteration, histologic changes, such as tumor cell apoptosis, may occur earlier during the treatment [6]. Thus, it would be of considerable value for us to find a sensitive and non-invasive method to evaluate the therapy response.

Molecular ultrasound imaging is a promising technique for non-invasive evaluation of tumor response to anticancer therapy, with the advantage of high spatial resolution, real-time imaging, low cost, and lack of ionizing irradiation [9]. Generally, anticancer strategies can lead to cancer cell killing and attenuate the tumor size, so that the non-invasive imaging of cell death events, especially cell apoptosis, has the potential predictive response to anticancer therapy [10]. An important molecular marker for apoptosis is Annexin V, which is a calcium-dependent phosphatidylserine-binding protein [11]. Ultrasound targeted imaging for apoptosis with Annexin V would be of great value for imaging cancer cell early death events. Thus, ultrasound molecular imaging targeted apoptosis could be useful in monitoring trastuzumab treatment effect in patients with Her-2–positive breast cancer. The aim of our study is to explore a valuable ultrasound imaging method in a preclinical model for the early assessment of breast cancer targeted therapy.

Materials and Methods

Cell Culture

The human breast cancer cell line SK-BR-3 (Her-2 positive), obtained from the Chinese Academy of Sciences Cell Bank, was cultured in Dulbecco's modified Eagle's medium, 10% FBS (Hyclone), and 1% L-glutamine. The cell line was grown in a 5% CO_2 incubator at 37 °C. All cell number assays were determined with a hemocytometer and trypan dye exclusion.

Targeted Nanobubble Preparation

Perfluoropropane-filled nanobubbles (NBs) were made from an amphiphilic biomaterial, biotin–poly(ethylene glycol)–poly(lactic-co-glycolic acid)–poly(ethylene glycol)–biotin. The poly(ethylene glycol) and poly(lactic-co-glycolic acid) were obtained from Rebone and Daigang Biomaterials Company (Shanghai, China). Briefly, biotin–poly(ethylene glycol)–poly(lactic-co-glycolic acid)–poly(ethylene glycol)–biotin was dissolved in dichloromethane at a final concentration of 100 mg/ml. The solution was poured into physiological saline (0.9%) and stirred at 10000 rpm for 5 minutes to acquire solution A. Solution A was subsequently poured into polyvinyl alcohol (Hengrui Chemical Industry Co, Ltd, Tianjin, China) aqueous solution (2.0 wt %) and stirred at 10000 rpm under a vacuum to get rid of dichloromethane. NB solution (1 mg/ml) was co-cultured with streptavidin for 24 hours at 4°C to get streptavidin-coated NBs. Targeted NBs were prepared by incubating these streptavidin-coated NBs with biotinylated Annexin V (Annexin V, 67 kDa; Abcam, Shanghai, China) at 4 °C for 20 minutes. Unconnected Annexin V was removed by centrifugation. The NB power was required after lyophilization and enveloped into a via filled with perfluoropropane. Before usage, the NBs were diluted using physiological saline (0.9%) to a total volume of 1.0 ml and a concentration of 50 mg/ml. A dynamic light scattering particle size analyzer (Brookhaven, INNDVO300/BI900AT) was used to determine the size of NBs. The mean diameter of NBs was 586 ± 6.0 nm (Figure 1).

In Vitro Studies

In the *in vitro* study, breast cancer SK-BR-3 cells were plated at 1×10^6 cells onto six-well plates for 24 hours. Treatment group was administrated by 20 μl of trastuzumab (10 μg/ml), and the control one was treated with 20 μl of phosphate-buffered saline for 30

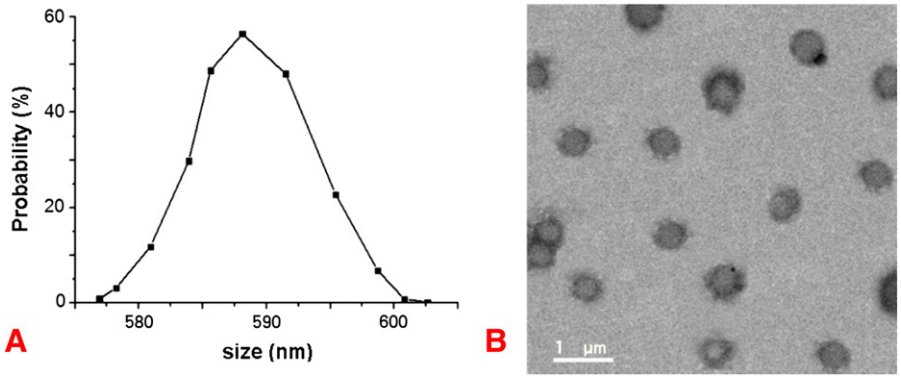

Figure 1. (A) The size distributions of targeted NBs were shown in the line graph (mean diameter of NB, 586 ± 6.0 nm). (B) The NB images were shown under the TEM (Philips EM400ST; scale bar, 1 μm).

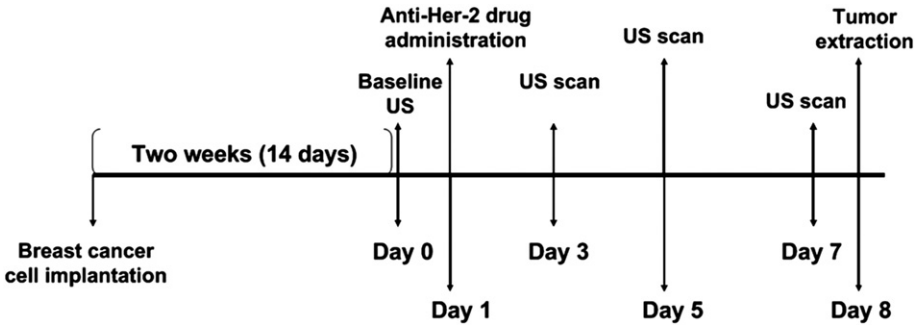

Figure 2. The time line demonstrated the experimental processes of the time points, when we performed tumor implantation (lasting for 14 days), anti–Her-2 drug dosing (day 1), contrast ultrasound targeted imaging (days 3, 5, and 7), and tumor extraction (day 8).

minutes. We then added 2.5 mol of $Cacl_2$ (100 μl) to each cell culture at room temperature overnight. Fluorescein isothiocyanate (FITC)–labeled Annexin V–NBs (purchased from Abcam; 5×10^6 NB per well) were incubated with SK-BR-3 cells (3×10^5 NB per well) in a 5% CO_2 incubator at 37°C for 60 minutes. SK-BR-3 cells were fixed with 4% polysorbate (Tianjin Umbrella Science and Technology, Co, Ltd, Tianjin, China) for 15 minutes and washed with phosphate-buffered saline three times and then blocked out by 5% BSA (Tianjin Umbrella Science and Technology, Co, Ltd) overnight.

The binding rates of FITC–Annexin V–NB with apoptotic cells were calculated under a fluorescence microscope. Meanwhile, cell nuclei co-stained with 4,6-diamidino-2-phenylindole (DAPI) were shown in Figure 3*B*, and cells with pyknosis or lumpy nucleus fragments were considered as apoptosis. For calculating binding rate,

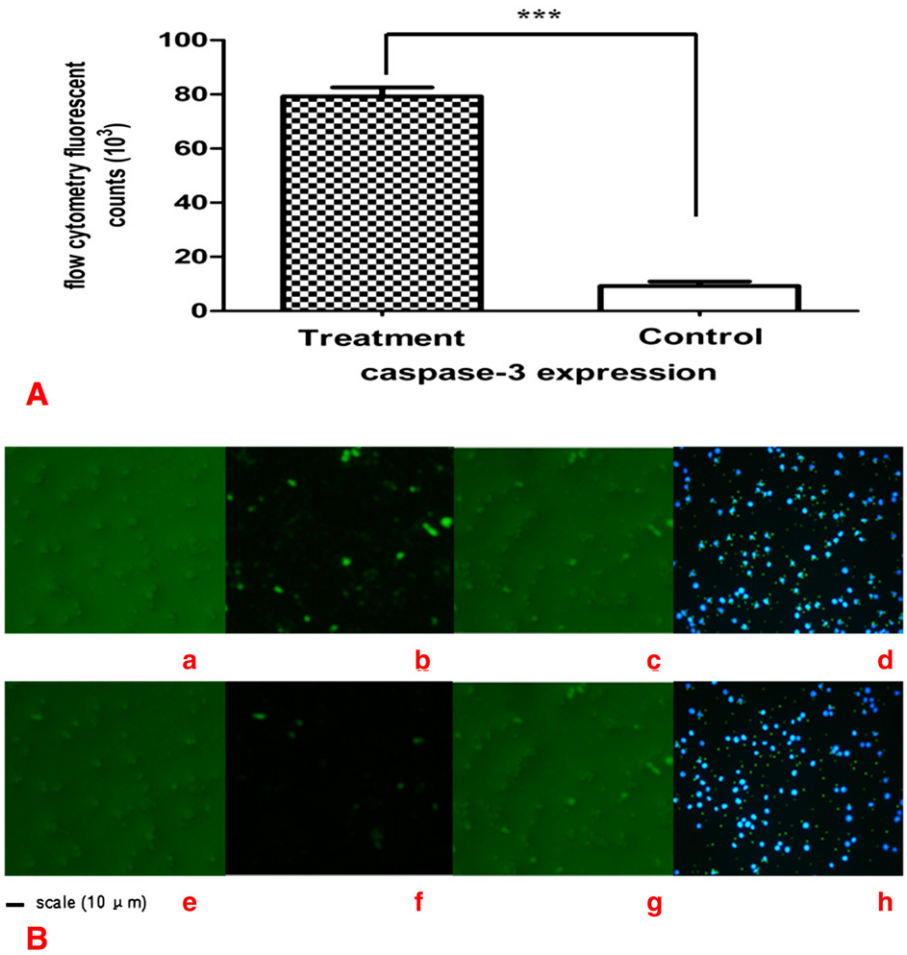

Figure 3. (A) *In vitro* data showing caspase-3 expressions in the treatment and control groups with flow cytometric mean fluorescent counts (***$P < .01$). (B) This figure demonstrated the fluorescence microscope images of SK-BR-3 cell (a and e), FITC–Annexin V–NB (b and f), and FITC–Annexin V–NB attached to SK-BR-3 cell (c and g) and cell nucleus stained with DAPI (d and h) in the treatment and control groups (scale bar, 10 μm). The binding rate of apoptotic cells (d and h) with FITC–Annexin V–NB attached in the treatment and control groups was calculated according to the methods mentioned.

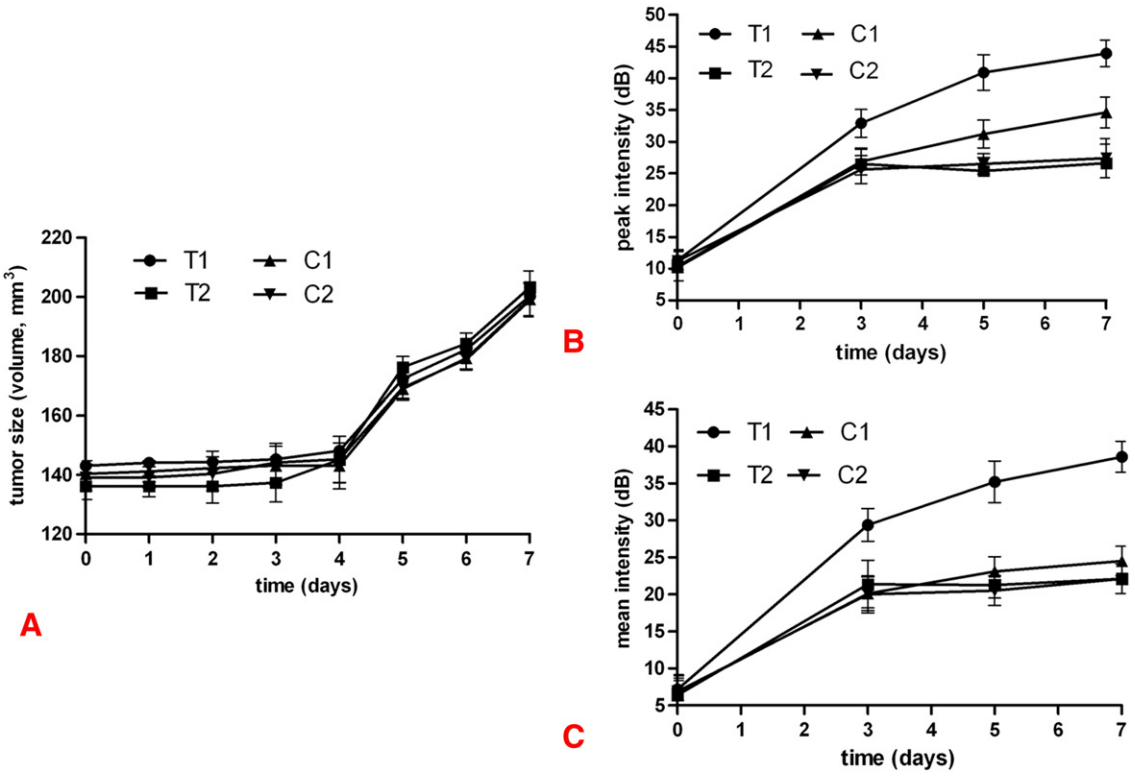

Figure 4. (A) There was no significant difference in tumor sizes from day 0 to day 7 in the treatment and control groups ($P = .98$), indicating that tumor size was not an indicator in early tumor response to anti–Her-2 drug. (B, C) TIC results showed that there were significantly stronger mean and peak intensities in the treatment group detected by targeted NBs (T1 group) compared to those in the other three groups (T2, C1, and C2 groups; $P = .001$; T1 group: the treatment group with NB–Annexin V; C1 group: the control group with NB–Annexin V; T2 group: the treatment group with NB-IgG (non-targeted NB); C2 group: the control group with NB-IgG).

two to three NBs binding one cell per 10 random microscopic fields were seen as positive in our study. Then, cells were stained by using caspase-3 antibody (Santa Cruz Biotechnology, Inc, Dallas, TX) by immunohistochemistry (IHC) to mark apoptotic cells. The apoptotic cells were analyzed by fluorescent counts using flow cytometry (Gallios Flow Cytometer; Beckman Coulter, Inc, Brea, CA).

Animal Preparation and In Vivo Studies

Animal experiments were approved by the Institutional Ethical Board of Tianjin Cancer Hospital (Tianjin, China). BALB/c nude mice were obtained from Tianjin Medical University (Tianjin, China). As a preparatory experiment, SK-BR-3 cells (2×10^6) were implanted in two mammary fat pads of each mouse ($n = 2$). The two different diameters (a and b) of tumors were measured, and the tumor volumes were calculated by the formula $V = ab^2/2$. The duration time lasted 2 weeks after implantation. Xenograft tumors ($n = 20$; the mean diameter was 6.1 ± 0.6 mm) in 10 mice were used for measuring the distribution of tumor vascular endothelial gaps. The mice were anesthetized with 0.5% pentobarbital sodium through intraperitoneal route. The tumors were extracted and fixed in 3% paraformaldehyde and 1% glutaraldehyde for 48 hours at 4°C. The samples (0.9 ± 0.06 mm^3) were embedded in Epon 812 (Haide Biotech Company, Beijing, China) and then sliced into 50-nm sections by ultramicrotome. The slices were observed to measure the size of gaps between tumor endothelial cells under a transmission electron microscope (TEM; Philips EM400ST).

In our following study, 40 mice were separated into four different groups ($n = 10$ per group). Treatment groups were T1 (trastuzumab treated + NB–Annexin V) and T2 (trastuzumab treated + NB-IgG); the control groups were C1 (NB–Annexin V only) and C2 (NB-IgG only). After a 14-day implantation (the mean diameter was 6.4 ± 0.7 mm; the average tumor size was 139.7 ± 5.2 mm^3), targeted NBs were intravenously injected (1×10^8 NBs per mouse in a 0.1-ml dose consisting of 0.05 ml of NBs and 0.05 ml of saline) in the tail vein (T1 and C1 groups) after the treatment.

Treatment Protocol

Trastuzumab (Herceptin; Genentech, South San Francisco, CA) was given to two treatment groups on day 1. The dosage was 0.5 mg (20 mg/kg) diluted with saline to 200 μl through intraperitoneal injection for each mouse in the treatment groups (T1 and T2 groups). Control groups (C1 and C2 groups) received a 200-μl intraperitoneal dose of saline.

Ultrasound Molecular Imaging

Ultrasound targeted imaging was performed *in vivo* on day 0 for baseline scanning and after the treatment for 3 days at three different times (days 3, 5, and 7) and was repeated three times a day (1, 6, and 12 hours; Figure 2). The skin above or around the tumor was shaved before imaging session. After mice were anesthetized, ultrasound imaging was performed with an iU22 scanner (Phillip Medical Systems, Andover, MA) using an L12-5 high-frequency linear transducer for grayscale imaging and an L9-3 transducer for contrast ultrasound imaging. Contrast dual-image model settings were optimized as follows: mechanical index was 0.06 and the frame rate was 11 Hz. The ultrasound

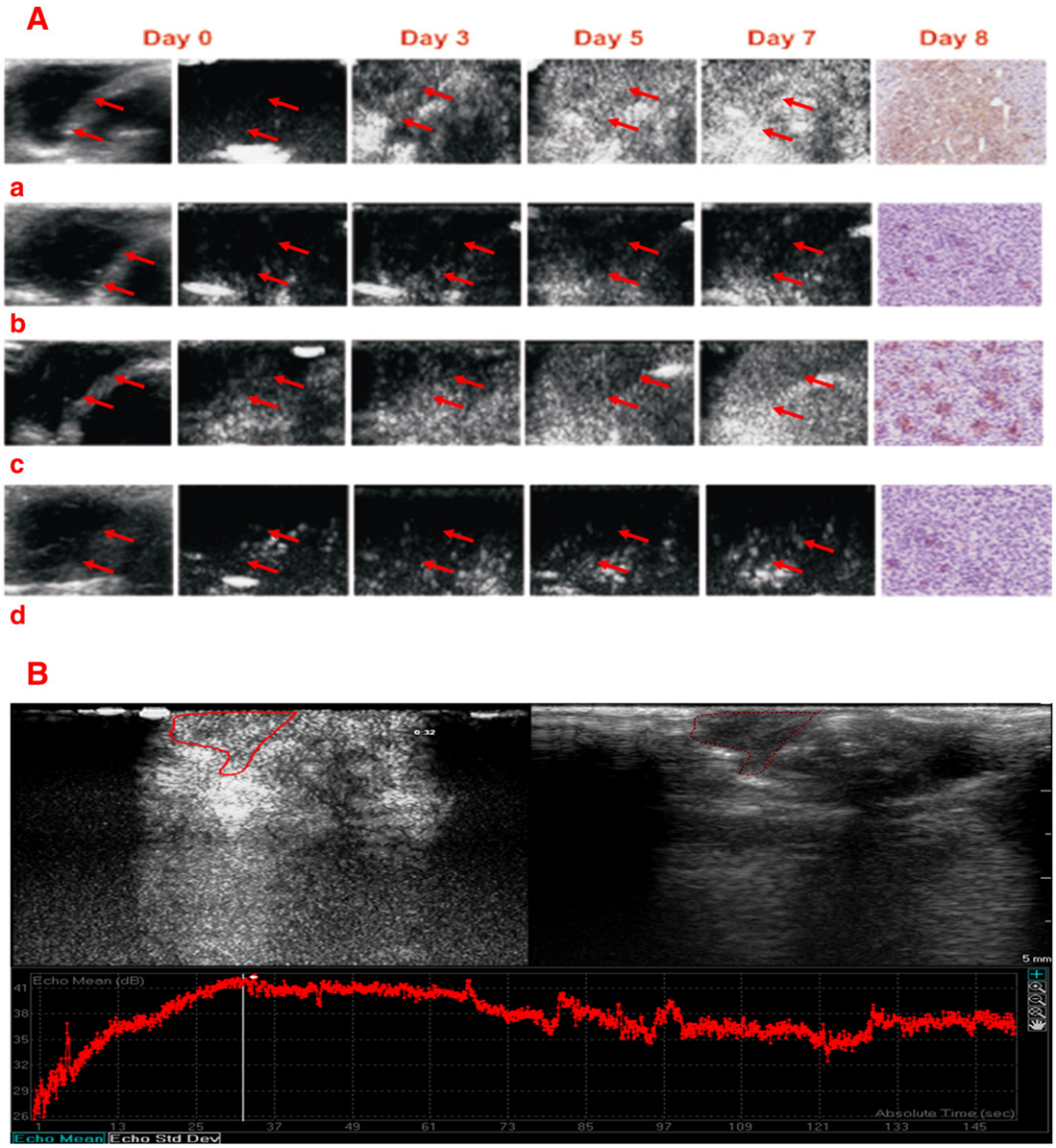

Figure 5. (A) On day 0, contrast ultrasound dual-image mode showed the baseline scanning (left: a contrast image; right: a grayscale image). From day 3 to day 7, ultrasound contrast imaging (60 minutes after NB injection) demonstrated a significant increase in the intratumoral perfusions (double red arrow showing) in the treatment group with NB–Annexin V (T1 group) (a) compared to those in the other three groups (T2, C1, and C2 groups) (b, c, and d). On day 8, the mouse tumors were excised and then stained by caspase-3 antibody (tumor cells immunostained brown and original magnification, ×200). This figure also showed the positive correlation between NB perfusions in these groups and caspase-3–positive expressions in tumor samples. (B) The contrast ultrasound dual image (left: a grayscale image; right: a contrast image) showed that ROI was an irregular red area within the mouse tumor (the figure above). TIC (the figure below) indicated that the peak intensities of ROI were 42.5 ± 4.8 dB and the mean intensities were 35.2 ± 3.5 dB, which were calculated by the QLAB software.

probe was placed at the center of the tumor at the largest transverse cross section. At least three probe planes were used to present tumors for calculating tumor volumes.

A dose of 100 μl targeted contrast agents diluted by saline was intravenously injected through the tail vein. Thirty seconds after the injection, contrast harmonic imaging was acquired to observe the contrast echoes from NBs. Ultrasound transmission was then paused for 60 minutes to allow targeted NBs to bind with apoptotic cells at targeted sites. The whole imaging process lasted 180 seconds to capture tumor perfusion of NB agents and was recorded on the hard disk of the scanner for post-imaging review. Images were then saved in the DICOM format. The regions of interests (ROIs) were given as the whole areas of tumors and analyzed by the QLAB software (Figure 5*B*). The change in NB signal intensity, the size of perfusion areas, and other parameters (arrival time, time to peak, and area under the curve) of the time-intensity curve (TIC) were also uploaded to QLAB for analysis. The average intensity of NBs was repeated three times at each point over the entire protocol. We calculated changes of these parameters before and during the study to compare their differences statistically.

IHC and Imaging Comparison

At the end of the protocol (day 8), mice were killed, and tumor samples were excised, fixed in formalin solution, embedded in

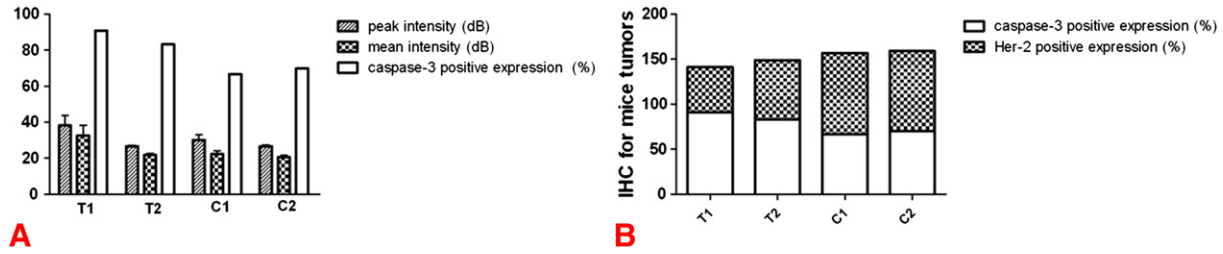

Figure 6. (A) Comparing the peak or mean intensities with the percentage of caspase-3–positive expressions in mouse tumors among these four groups, the data demonstrated significant correlations among these parameters ($r = 0.78$, $P = .038$; $r = 0.69$, $P = .042$, respectively). (B) The percentage of Her-2 and caspase-3–positive expressions in mouse tumors among the four groups showed that there was an adverse trend between Her-2 expressions and caspase-3 expressions during the anti–Her-2 drug treatment. This figure indicated that there have been tumor responses for anti–Her-2 drug therapy *in vivo*, which led to tumor Her-2 expressions decreasing and tumor cell apoptosis increasing (T1 group: the treatment group with NB–Annexin V; C1 group: the control group with NB–Annexin V; T2 group: the treatment group with NB-IgG (non-targeted NB); C2 group: the control group with NB-IgG.)

paraffin, and then sliced into 5-μm sections using a microtome. Samples were stained by hematoxylin and eosin to visualize the tumor necrosis within different groups. The anti-murine caspase-3 p11 antibody (Santa Cruz Biotechnology, Inc) was used for histochemistry to detect the cell apoptosis in tumors (Figure 5*A*).

The immunoreaction for caspase-3 and Her-2 (anti–Her-2 antibody; Abcam) in tumor cells was determined by two pathologists (P.Y. and C.R.F.), and the consensus was reached for the final diagnosis. The scores and percentage of tumor cells stained are described as follows [5,6]: no positive cells (–), 1% to 10% of the cells stained (+), 11% to 50% of cells stained (++), and 51% to 100% of the cells stained (+++). We then calculated the percentage of number of mice with positive caspase-3 and Her-2 expression in each group and described them by bars. Comparison with the average mean and peak NB intensities analyzed by the software after the treatment was carried out to find the correlation between NB intensities and IHC results.

Statistical Analysis

Statistical analyses were performed with SPSS statistical software package (17.0 version; SPSS Inc, Chicago, IL). Data were summarized as means ± standard error. *In vitro*, count data were analyzed in the assessment of the intergroup comparison with a two-sample independent *t*-test. Analyses of mouse weight and tumor size or parameters of ultrasound imaging were compared between groups with multiple comparison in analysis of variance (Student-Newman-Keuls test or least significant difference procedure test). A correlation between histologic and imaging experimental data was performed by Pearson correlation test. A *P* value below .05 was considered significant.

Results

Characteristic of NBs and In Vitro Experiment

As Figure 1*B* showed, the NBs prepared before was well distributed and uniformed, which was described as a normal distributed curve (Figure 1*A*), and the mean sizes of NB was 586 ± 6.0 nm.

After the trastuzumab administration, the binding rate of targeted NB with human breast cancer apoptotic cells was higher than that of the control group (79.2 ± 3.3% *vs* 9.2 ± 1.7%, $P = .001$; Figure 3*B*). The average number of cells with caspase-3 expression in the treatment group increased significantly compared to that of the control one [$(82.6 \pm 3.5) \times 10^3$ and $(21.4 \pm 2.3) \times 10^3$, respectively; Figure 3*A*].

In Vivo Experiment and Histologic Analysis

All mice were alive during the whole experiment. In the preparatory study, we observed the tumor slices under the TEM and calculated the mean sizes of gaps between vascular endothelial cells (865 ± 5.2 nm; range, 630-1325 nm) for 20 xenograft tumors. This result indicated that average gap sizes between tumor vascular endothelial cells were larger than our NB mean sizes (586 ± 6.0 nm) in our mouse model.

As the time line in Figure 2 showed, we processed the following experiment and observed that there were no statistical differences in the average weights of mice within four groups on day 0 ($P = .76$) and day 7 ($P = .79$). As for tumor sizes, the data indicated no differences among four groups from day 0 to day 7 during the whole treatment process ($P = .98$; Figure 4*A*). Histologic analysis showed that there were no significant differences in the percentage of necrotic areas of samples between treatment (TI and T2) and control groups (C1 and C2; $P = .21$). At the end of treatment, anti–Her-2 therapy response was investigated by IHC analyses of Her-2 and caspase-3 expression in excised tumors. The data showed that the percentages of Her-2–positive expression in mouse tumors in the two treatment groups (TI and T2; 54.5% and 66.7%) were lower than the control ones (91.2% and 80%, respectively; Figure 6*B*). This indicated that there was effective treatment in mouse xenograft models (T1 and T2 groups) and the trastuzumab treatment also induced apoptosis cells in these tumors. Thus, the percentages of caspase-3–positive expression in mouse samples in the two treatment groups (TI and T2) were higher than those of the control groups (C1 and C2; 90.0% and 83.3% *vs* 66.7% and 70%, respectively; Figure 6*A*).

Ultrasound Targeted Imaging and Histologic Result Correlation

The ultrasound contrast imaging detected NB signals in *in vivo* models after 60 minutes from the injection of NB through the mouse tail vein, and this process was carried out under different time points (days 0, 3, 5, and 8; Figure 5*A*). Then, ultrasound imaging software analyses indicated that the average mean intensities of targeted bubbles in ROIs (Figure 5*B*) in the T1 group were significantly higher than those in the other three groups (T2, C1, and C2; $P = .001$; Figure 4*C*). However, there were no differences within the three

groups (T2, C1, and C2 groups), when one group was compared to other three groups (T2 *vs* T1 + C1 + C2, $P = .74$; C1 *vs* T1 + T2 + C2, $P = .51$, and C2 *vs* T1 + T2 + C1, $P = .33$, respectively). As for peak intensities of intratumor microbubble perfusion, they were also higher in the T1 group than those in the other groups (T2, C1, and C2; $P = .00$), but there were no differences within T2, C1, and C2 groups ($P = .43$, .96, and .42, respectively; Figure 4*B*). The correlations between the mean and peak intensities of ultrasound imaging and caspase-3 expression of the tumor samples were statistically significant in all four groups after the treatment ($r = 0.78$, $P = .038$; $r = 0.69$, $P = .042$, respectively; Figures 5*A* and 6*A*).

Discussion

Trastuzumab has been used in the treatment of Her-2–positive metastatic breast cancer over one decade [4,7,8]. Although it has great affinity for Her-2 and low toxicity, about 70% of patients do not respond to this treatment [12]. Therefore, early identification of patients who would benefit from trastuzumab can avoid additional cost for patients [6]. Traditional imaging and fluorescent *in situ* hybridization have been viewed as the "gold standard" techniques for predicting the treatment response, but they are expensive and not real-time systems [4,13,14]. Our study intended to investigate the usage of ultrasound molecular imaging techniques to evaluate the response to trastuzumab therapy in Her-2–positive breast cancer in the tumor xenograft model.

Dynamically monitoring the tumor inner change, such as tumor cell apoptosis during treatment, could be an early indicator of breast cancer response to trastuzumab [15]. An apoptosis marker, Annexin V, has been labeled with FITC and coupled to magnetic nanoparticles to identify apoptotic cells [22,24]. In addition, there were various methods to design targeted apoptosis probes to detect tumor cell apoptosis. Previous studies used biotin/streptavidin interactions to conjugate targeting ligands, such as $\alpha_v\beta_3$ integrin, P-selectin, or vascular endothelial growth receptor 2, to image tumor angiogenesis, or to evaluate the antiangiogenic therapy response of tumors [16–18]. In our targeted apoptosis NB design, streptavidin-based bubbles binding to biotin–Annexin V were also used to dynamically detect tumor apoptotic cells during treatment *in vitro* and *in vivo*. These targeted bubbles with nanolevel diameters (less than 600 nm) can easily pass through the gaps between the tumor's new microvascular endothelial cells (865 ± 5.2 nm, tested in the preparatory study) to adhere to the surface of tumor apoptotic cells in our tumor xenograft model. In the imaging study, we tested signals of NBs at 60 minutes after the injection. According to previous reports [17,19], it would be of enough time for bubbles to bind to tumor cells through vessels. Thus, it is possible for us to use these targeted NBs to detect tumor apoptotic cells *in vivo*.

First, for seeking the binding ability of targeted NB with targeted cells *in vitro*, we found that NB–Annexin V bound to trastuzumab-treated cells significantly better than to control (buffer-treated) cells, which is confirmed by DAPI-stained nucleus test and caspase-3–positive expression. After preparing the breast cancer–bearing mice, we performed ultrasound targeted imaging to assess the early response to anti–Her-2 drugs in breast cancer. We noted that the change of tumor sizes has no difference between treatment groups and control ones during the whole experiment. However, targeted apoptosis NB intensities in tumors (mean and peak intensity) detected by ultrasound contrast imaging became stronger after the anti–Her-2 drug treatment. This phenomenon indicated that tumor cell apoptosis scanned by ultrasound targeted apoptosis imaging happened earlier than the change of tumor size during the treatment.

For further investigating the anti–Her-2 drug efficiency, we stained all excised tumors in the four groups by anti–Her-2 antibody. The results showed that there was lower Her-2–positive percentage in mouse tumors among treatment groups than that in control groups. This indicated that breast tumors *in vivo* have good pathologic response to the anti–Her-2 drug. Furthermore, our ultrasound imaging results facilitated the detection of tumor response of trastuzumab before excising mouse tumors.

Moreover, our study also demonstrated that the intensity of targeted NBs was significantly associated with caspase-3 expressions of tumor samples at the end of experiment. Therefore, ultrasound targeted imaging with NB–Annexin V could be a good tracer to indicate cell apoptosis events and early prediction of trastuzumab therapy outcome in breast cancer. In addition, a large number of data strongly suggested that apoptosis in tumors after treatment happened earlier than cell proliferation and glucose metabolism did [9,20,21]. Thus, targeted apoptosis molecular imaging could be a feasible indicator for therapy response of tumors.

In conclusion, targeted apoptosis ultrasound imaging will be a promising and non-invasive technique to the early prediction of breast cancer response to anti–Her-2 therapy. More targeted ultrasound imagings should be investigated to early evaluate the therapy outcome of cancers on the platform of ultrasound molecular imaging.

Acknowledgments

We are also grateful to R.S. for his valuable suggestion on this manuscript.

References

[1] He J, Chen W, editors. Chinese Cancer Registry Annual Report 2012 by National Cancer Center & Disease Prevention and Control Bureau, Ministry of Health. Beijing, China: Military Medical Science Press; 2012.

[2] Moasser MM (2007). Targeting the function of the HER2 oncogene in human cancer therapeutics. *Oncogene* **26**(46), 6577–6592.

[3] Demonty G, Bernard-Marty C, Puglisi F, Mancini I, and Piccart M (2007). Progress and new standards of care in the management of HER-2 positive breast cancer. *Eur J Cancer* **43**(3), 497–509.

[4] Brollo J, Curigliano G, Disalvatore D, Marrone BF, Criscitiello C, Bagnardi V, Kneubil MC, Fumagalli L, Locatelli M, and Manunta S, et al (2013). Adjuvant trastuzumab in elderly with HER-2 positive breast cancer: a systematic review of randomized controlled trials. *Cancer Treat Rev* **39**(1), 44–50.

[5] Wei X, Li Y, Zhang S, Zhu Y, and Fan Y (2011). Experience in large-core needle biopsy in the diagnosis of 1431 breast lesions. *Med Oncol* **28**(2), 429–433.

[6] Shah C, Miller TW, Wyatt SK, McKinley ET, Olivares MG, Sanchez V, Nolting DD, Buck JR, Zhao P, and Ansari MS, et al (2009). Imaging biomarkers predict response to anti-HER2 (ErbB2) therapy in preclinical models of breast cancer. *Clin Cancer Res* **15**(14), 4712–4721.

[7] Boekhout AH, Beijnen JH, and Schellens JH (2011). Trastuzumab. *Oncologist* **16**(6), 800–810.

[8] Tortora G (2011). Mechanisms of resistance to HER2 target therapy. *J Natl Cancer Inst Monogr* **2011**(43), 95–98.

[9] Belhocine T, Steinmetz N, Hustinx R, Bartsch P, Jerusalem G, Seidel L, Rigo P, and Green A (2002). Increased uptake of the apoptosis-imaging agent ^{99m}Tc recombinant human Annexin V in human tumors after one course of chemotherapy as a predictor of tumor response and patient prognosis. *Clin Cancer Res* **8**(9), 2766–2774.

[10] Schoenberger J, Bauer J, Moosbauer J, Eilles C, and Grimm D (2008). Innovative strategies in in vivo apoptosis imaging. *Curr Med Chem* **15**(2), 187–194.

[11] Koopman G, Reutelingsperger CP, Kuijten GA, Keehnen RM, Pals ST, and van Oers MH (1994). Annexin V for flow cytometric detection of phosphatidylserine expression on B cells undergoing apoptosis. *Blood* **84** (5), 1415–1420.

[12] Murphy CG and Modi S (2009). HER2 breast cancer therapies: a review. *Biologics* **3**, 289–301.

[13] Morse DL and Gillies RJ (2010). Molecular imaging and targeted therapies. *Biochem Pharmacol* **80**(5), 731–738.

[14] Jennings BA, Hadfield JE, Worsley SD, Girling A, and Willis G (1997). A differential PCR assay for the detection of c-erbB 2 amplification used in a prospective study of breast cancer. *Mol Pathol* **50**(5), 254–256.

[15] Specht JM and Mankoff DA (2012). Advances in molecular imaging for breast cancer detection and characterization. *Breast Cancer Res* **14**(2), 206.

[16] Sorace AG, Saini R, Mahoney M, and Hoyt K (2012). Molecular ultrasound imaging using a targeted contrast agent for assessing early tumor response to antiangiogenic therapy. *J Ultrasound Med* **31**(10), 1543–1550.

[17] Anderson CR, Hu X, Zhang H, Tlaxca J, Declèves AE, Houghtaling R, Sharma K, Lawrence M, Ferrara KW, and Rychak JJ (2011). Ultrasound molecular imaging of tumor angiogenesis with an integrin targeted microbubble contrast agent. *Invest Radiol* **46**(4), 215–224.

[18] Warram JM, Sorace AG, Saini R, Umphrey HR, Zinn KR, and Hoyt K (2011). A triple-targeted ultrasound contrast agent provides improved localization to tumor vasculature. *J Ultrasound Med* **30**(7), 921–931.

[19] Kong G, Braun RD, and Dewhirst MW (2000). Hyperthermia enables tumor-specific nanoparticle delivery: effect of particle size. *Cancer Res* **60**(16), 4440–4445.

[20] Manning HC, Merchant NB, Foutch AC, Virostko JM, Wyatt SK, Shah C, McKinley ET, Xie J, Mutic NJ, and Washington MK, et al (2008). Molecular imaging of therapeutic response to epidermal growth factor receptor blockade in colorectal cancer. *Clin Cancer Res* **14**(22), 7413–7422.

[21] Van de Wiele C, Lahorte C, Vermeersch H, Loose D, Mervillie K, Steinmetz ND, Vanderheyden JL, Cuvelier CA, Slegers G, and Dierck RA (2003). Quantitative tumor apoptosis imaging using technetium-99m–HYNIC annexin V single photon emission computed tomography. *J Clin Oncol* **21**(18), 3483–3487.

[22] Schellenberger EA, Sosnovik D, Weissleder R, and Josephson L (2004). Magneto/optical annexin V, a multimodal protein. *Bioconjug Chem* **15**(5), 1062–1067.

[23] Deshpande N, Pysz MA, and Willmann JK (2010). Molecular ultrasound assessment of tumor angiogenesis. *Angiogenesis* **13**(2), 175–188.

[24] Vermes I, Haanen C, and Reutelingsperger C (2000). Flow cytometry of apoptotic cell death. *J Immunol Methods* **243**(1–2), 167–190.